Supplementary Material of "SIGMA: A Physics-Based Benchmark for Gas Chimney Understanding in Seismic Images"

Bao Truong[1], Quang Nguyen[1], Baoru Huang[5,*], Jinpei Han[2], Van Nguyen[1], Ngan Le[3], Minh-Tan Pham[4], Doan Huy Hien[1], Anh Nguyen[5]

[1]FPT Software AI Center [2]Imperial College London [3]University of Arkansas

[4]University of South Brittany [5]University of Liverpool [*]Corresponding author

https://airvlab.github.io/sigma

SUMMARY

This Supplementary Material provides extra material for the paper "*SIGMA: A Physics-Based Benchmark for Gas Chimney Understanding in Seismic Images*". The material is organized as follows:

- Section 1 defines seismic images and their importance in seismic imaging applications, along with an explanation of the concept of a gas chimney and its impact on seismic data interpretation.
- Section 2 describes what velocity models are, how they represent subsurface properties, their role in seismic imaging, and why they are crucial for generating realistic gas chimney seismic data instead of directly adding noise to seismic images.
- Section 3 provides an analysis of the reliability of generated seismic images.
- Section 4 details the user study performed to validate the generated seismic images, including detailed results, analysis of failure cases and insights.
- Section 5 describes the detail experimental setup for evaluating the SIGMA dataset on related tasks.
- Section 6 discusses some interesting future directions.

1. Seismic Imaging

As outlined in Section 2 of the main paper, we provide a more detailed explaination of the concepts of seismic image and gas chimney, along with their problems.

What is seismic image? In surface exploration geophysics, a *seismic image* refers a two- or three-dimensional representation of the subsurface derived from reflected seismic wavefields [6, 24]. More formally, seismic imaging is the numerical process of creating an image of the subsurface from reflections recorded at the subsurface. The primary significance of seismic images in geophysical applications lies in their ability to reveal subsurface geological structures with high resolution. These images serve as essential tools for surveying and decision-making processes in the oil and gas industry, where understanding the geometry and properties of the subsurface directly influences drilling strategies, risk assessment, and reservoir management [19].

What is gas chimney? Gas chimneys are commonly seen in seismic images, and are vertical or near-vertical disturbed zones in seismic data associated with the migration of fluids or gases upward through the sedimentary column [3, 15]. They appear in seismic images as zones of disrupted or attenuated reflections, often marked by chaotic, diffused amplitude patterns or zones of weak coherence [11, 15]. The underlying mechanism usually involves fluid or gas escaping from subsurface reservoirs. As it moves upward through fracture pathways, it creates variations in velocity and attenuation within the overlying layers [5].

Why is it important to understand gas chimneys? In seismic imaging, the presence of gas saturation, along with scattering, attenuation, tends to degrade the seismic response both within and beneath the chimney zones [15]. Arising from the complex nature of gas chimney formation and its impact on the seismic signals, the task of detecting, accurately mapping gas chimney zones, and reconstructing seismic features presents significant technical challenges, often requiring extensive time, effort, and financial resources. Despite these obstacles, efforts dedicated to understanding gas chimneys are critical, as they provide invaluable insights into subsurface fluid dynamics, such as hydrocarbon migration, leakage, and the processes of reservoir recharge [11, 18]. The accurate identification of gas chimney zones are fundamental for improving the reliability of seismic imaging, as well as for ensuring precise interpretation of subsurface data. These factors highlight the complexity of gas chimney characterization and underscore the

need for further research in the field to improve gas chimney understanding. Moreover, the insights gained from improving gas chimney understanding methods will contribute to a broader impact that could benefit various other fields within the computer vision community.

2. Velocity Models

What is a velocity model? In seismic imaging, a velocity model provides a quantitative description of seismic-wave propagation through subsurface geological formations. It defines the seismic velocity at each spatial point within the subsurface, which is essential for accurately interpreting seismic data. Velocity model can take the form of a 1D depth-varying profile, a 2D map, or a full 3D volume, depending on survey scale, and data availability [20].

Why are velocity models essential and fundamental for realistic synthetic seismic data? Velocity models are fundamental to the seismic imaging workflow: they serve as prerequisite inputs for migration algorithms and are required to correctly position and reconstruct subsurface reflectors. Inaccurate velocity models often lead to degraded imaging quality, making it difficult to recover detailed and reliable subsurface structures [1]. In physical terms, a velocity model reflects the subsurface's physical properties that govern wave propagation, and is therefore essential for reproducing realistic seismic images. For this reason, the velocity model plays a central role in the synthetic data generation process, serving as the ground truth that defines the complexity and fidelity of the resulting wavefield.

3. Reliability of SIGMA Dataset

Why don't we simply add random noise to a normal seismic image to simulate a gas chimney? As detailed in Section 1, gas chimney occurrences in the subsurface can significantly affect the seismic imaging process, leading to noisy, degraded, blurred, or low-coherence regions in the final seismic image [3, 15]. Thus, a gas–chimney–affected seismic image can be viewed as a degraded version of a normal seismic image. In the natural-image domain, numerous methods exist for simulating degradation or corruption of the original image such as the addition of Gaussian noise, application of low-level filter noise, or more sophisticated modeling approaches [4, 12, 27]. However, in seismic image domain, the presence of a gas-chimney phenomenon introduce a distinct form of degradation, as *it evolves over geological time through underlying physical processes*. Accordingly, we employ the velocity model as a physically grounded representation of the local subsurface, thereby enabling a modeling of the temporal evolution of the gas-chimney phenomenon. In our data generation framework, to generate a synthetic seismic image with gas chimney effects, we begin with an initial velocity model and apply gas chimney modeling through a physics-based simulation process, following the method in [2]. This framework enhances the reliability of our generated dataset, as the images are produced by modeling a physically meaningful phenomenon evolving over time, rather than by injecting random statistical noise into the original seismic image. As illustrated in Fig. 2, the gas chimney seismic image simulated by injecting Gaussian noise cannot show the seismic characteristics signature governed by rock physics and wave attenuation, instead only creating unstructured high-frequency noise that degrades the signal-to-noise ratio. Additionally, we provide extra samples generated by our framework in Fig. 1 to enable a better understanding.

Are 400 samples enough for the gas chimney understanding? Compared to traditional computer vision datasets with millions of images, our SIGMA dataset contains only 400 samples, making it relatively small in sample count. However, these 400 seismic image pairs span more than 1,600 km², providing a foundation for studying and understanding gas chimneys at the real-world scale. This coverage is notably larger than that of many available datasets in the field [7, 8, 13]. With our SIGMA dataset, the geographic range ensures a comprehensive representation of subsurface features, enabling detailed gas chimney surveys. In the context of gas chimney understanding, the variety of geological conditions and the large-scale coverage of the dataset significantly enhance its utility, the current dataset already serves as a strong foundation for addressing gas-chimney-related tasks. Furthermore, our study also provides an open framework for dataset generation, which allows for the scalable creation of additional data whenever high-quality velocity models are available. However, constructing such models remains a time-consuming and computationally intensive process; it requires solving a challenging Full Waveform Inversion task and demands domain experts to validate. Despite these constraints, our framework ensures that the dataset can continue to grow in both diversity and scale, supporting future advanced learning-based methods on seismic imaging data.

4. User Study Details

To assess how closely the generated seismic images resemble real data, we conducted a user study to evaluate their perceptual realism (see Section 4.4 of the Main Paper). Given the specialized nature of seismic imaging, the study involved 80 participants (ages 22–50), including 56 AI researchers and 24 geoscientists, all with substantial domain expertise. Each participant was presented with ten randomly shuffled and unlabeled seismic images (five real and five synthetic) and was asked to judge whether each image appeared to be a real seismic image. Fig. 3 illustrates two representative synthetic test cases: a successful example and a failure case (Fig. 3-a), along with the cor-

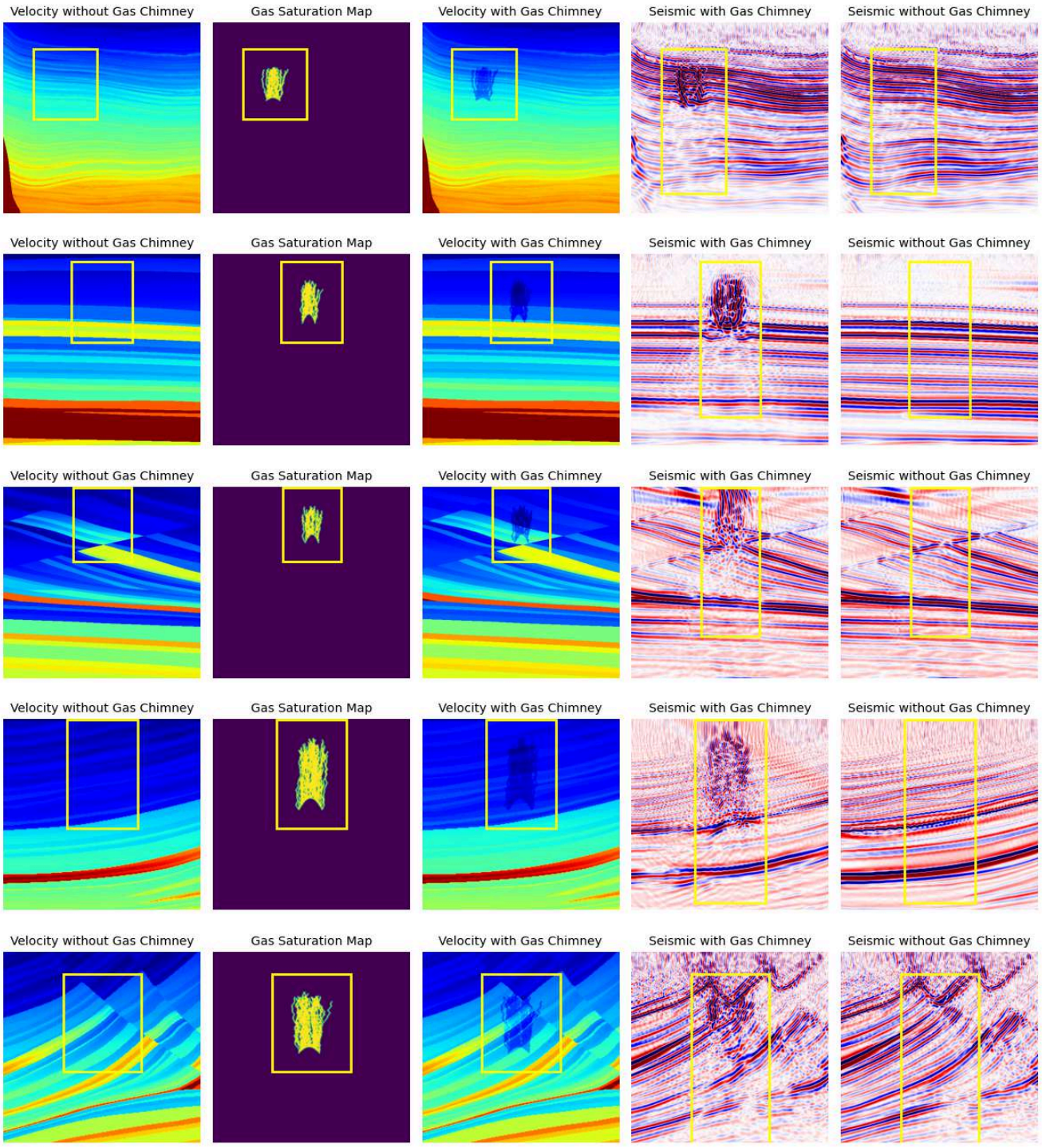

Figure 1. **Data samples.** We present more samples from our SIGMA, each sample consists of original velocity model, gas saturation map, velocity model with gas chimney, seismic with gas chimney effect image and ground-truth seismic image without gas chimney. The yellow bounding boxes highlight the differences between normal and gas-affected regions.

responding distribution of participant responses (Fig. 3-b). The failure case is readily explained by examining its degraded seismic textures, which appear blurred, noisy, and exhibit low contrast between adjacent layers, as highlighted

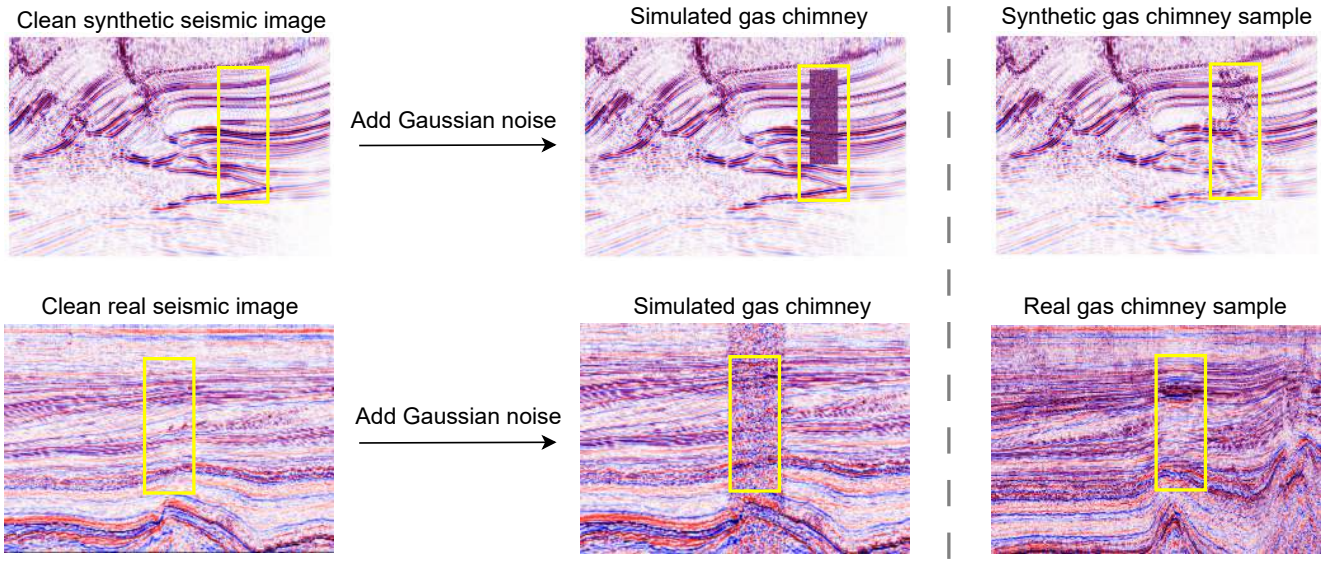

Figure 2. **Comparison of gas chimney generation methods.** We present the results of two approaches: a simple Gaussian noise injection and our physically grounded approach using velocity models to generate realistic synthetic seismic data. The yellow boxes highlight the areas where gas chimneys are localized.

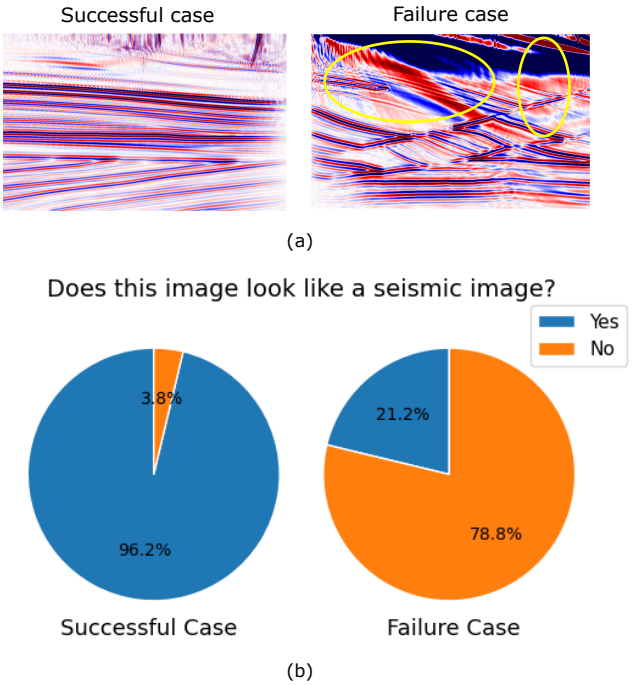

Figure 3. **Examples from our user study.** (a) Two synthetic test examples: a successful case and a failure case. Yellow-box annotations indicate regions where seismic texture is degraded or collapsed. (b) Pie charts summarize participants' responses for each sample across response categories, indicating the perceived realism of the synthetic images.

by the yellow annotations. All failure cases are manually checked and removed from our final data.

5. Experiment Details

In this section, we describe the training setup for the baselines in our benchmark, focusing on two main tasks: (*i*) gas chimney detection and (*ii*) gas chimney enhancement.

5.1. Gas Chimney Detection

Baseline and Training. We benchmark four recent methods for this task: FaultSEG [23], DualUNet [22], FaultFormer [21], and FaultViT [14], under a unified training pipeline based on the Dice loss function [17]. The Dice loss is defined as:

$$\mathcal{L}_{\text{Dice}} = 1 - \frac{2\sum_i p_i g_i + \epsilon}{\sum_i p_i + \sum_i g_i + \epsilon}, \tag{1}$$

where p_i and g_i represent the predicted and ground-truth labels at pixel i, and ϵ is a small constant for numerical stability, prevents division by zero. For a fair comparison, all models are trained for 300 epochs using the Adam optimizer with a momentum factor of 0.98. We adopt a cosine annealing learning rate scheduler to gradually reduce the learning rate from the initial value of 1×10^{-3} to 1×10^{-6}, which stabilizes convergence in the later training stages. A batch size of 8 is used for all experiments by utilizing three NVIDIA RTX 8000 GPUs.

Additional Visualization. As summarized in Table 2 of the main paper, we present a qualitative comparison in Fig. 4 for the detection task. The results show that all compared methods successfully capture the overall gas chimney structures. However, gas-chimney detection demands highly

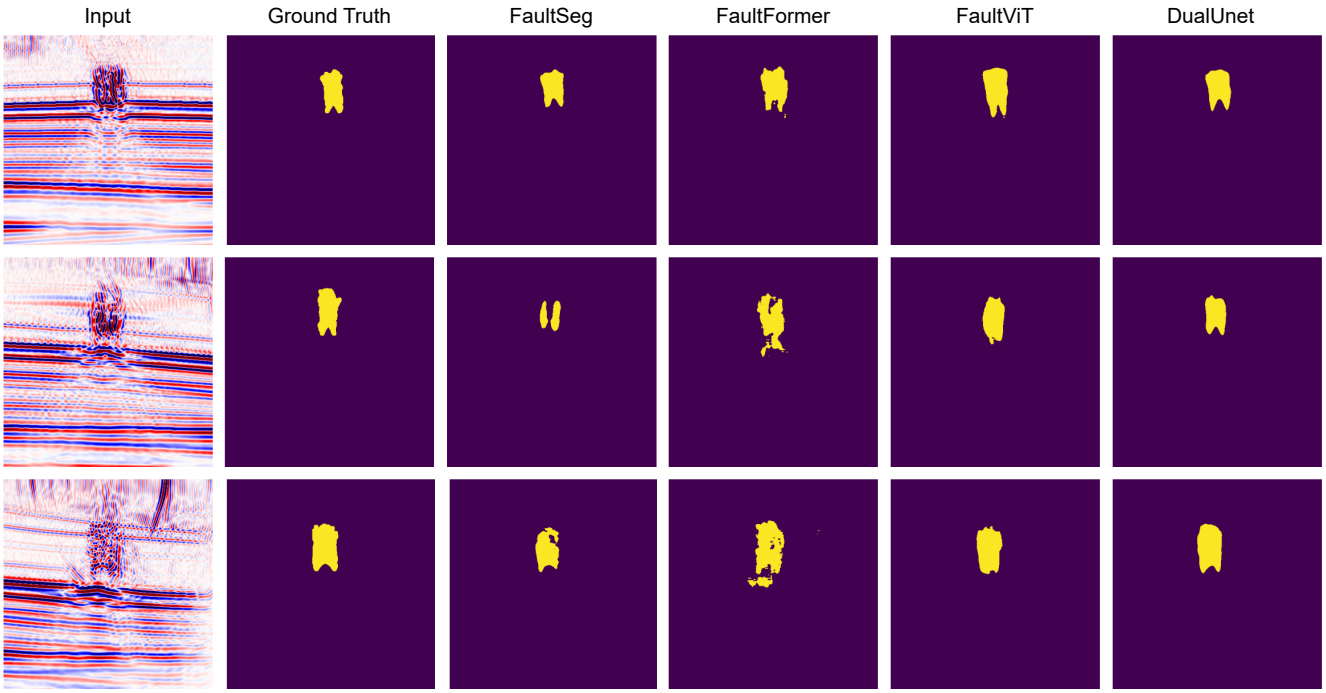

Figure 4. **Qualitative results on detection task.** We compare gas chimney mask outputs from different methods.

precise spatial localization, particularly around thin, irregular, or fragmented gas pathways. Although the predictions appear visually reasonable, detailed localization errors remain, highlighting the need for more advanced methods to achieve fine-grained gas chimney interpretation.

5.2. Gas Chimney Enhancement

Baseline and Training. In our experiment setup for enhancement task, we benchmark five recent methods: SeisResoDiff [26], SeisDDPM [10], SeisGAN [16], ConditionGAN [25], and SIST [9]. In GAN-based models, we adopt the Wasserstein Generative Adversarial Network with Gradient Penalty (WGAN-GP) to enhance training stability by enforcing a soft Lipschitz constraint on the discriminator (critic). The critic is optimized to maximize the difference between its outputs on real and generated samples, while the gradient penalty term regularizes the norm of its gradients along interpolated samples between real and synthetic data. The critic loss is defined as:

$$\begin{aligned}\mathcal{L}_D = \mathbb{E}_{\mathbf{z}\sim p(\mathbf{z})}\big[D(G(\mathbf{z}))\big] - \mathbb{E}_{\mathbf{x}\sim p_{\text{data}}}\big[D(\mathbf{x})\big] \\ + \lambda\, \mathbb{E}_{\hat{\mathbf{x}}\sim p(\hat{\mathbf{x}})}\Big(\|\nabla_{\hat{\mathbf{x}}} D(\hat{\mathbf{x}})\|_2 - 1\Big)^2,\end{aligned} \tag{2}$$

where $\hat{\mathbf{x}} = \epsilon\,\mathbf{x} + (1-\epsilon)G(\mathbf{z})$ and $\epsilon \sim \mathcal{U}(0,1)$, with λ being the gradient penalty weight. The generator loss aims to minimize the discriminator's ability to distinguish between real and generated samples, given by:

$$\mathcal{L}_G = -\mathbb{E}_{\mathbf{z}\sim p(\mathbf{z})}\left[D(G(\mathbf{z}))\right]\ . \tag{3}$$

For the conditional GAN model, the loss functions are extended by conditioning both the generator and discriminator on a label y, where y represents the degraded gas chimney version.

In diffusion-based models, the loss minimizes the mean squared error (MSE) between the predicted noise $\epsilon_\theta(\mathbf{x}_t, t)$ and the actual noise ϵ added during the forward process:

$$\mathcal{L}_{\text{diff}} = \mathbb{E}_{\mathbf{x}_0,\epsilon}\left[\|\epsilon_\theta(\mathbf{x}_t, t) - \epsilon\|^2\right]. \tag{4}$$

Finally, the learning-based method SIST [9] was trained using the MSE loss, following the same training strategy as the gas chimney detection task.

6. Future Works

We see several interesting directions for future work. First, we aim to contribute to the development of large-scale seismic foundation models by utilizing our dataset to improve generalization across diverse seismic phenomena. Additionally, we also plan to scale up the dataset by utilizing advanced full-waveform inversion methods to synthesize high-quality velocity models, which are essential for seismic imaging. Finally, we aim to propose effective methods for addressing the current challenges in gas chimney understanding, providing a more comprehensive solution to this challenging problem.

References

[1] Abdullah AlAli and Fatai Anifowose. Seismic velocity modeling in the digital transformation era: a review of the role of machine learning. *Journal of Petroleum Exploration and Production Technology*, 2022. 2

[2] Børge Arntsen, Lars Wensaas, Helge Løseth, and Christian Hermanrud. Seismic modeling of gas chimneys. *Geophysics*, 2007. 2

[3] C. Berndt. Focused fluid migration through sedimentary basins and its implications for gas hydrate formation. *Geofluids*, 2003. 1, 2

[4] Oleksandra Bielova, Ronny Hansch, Andreas Ley, and Olaf Hellwich. A digital image processing pipeline for modelling of realistic noise in synthetic images. In *CVPR Workshops*, 2019. 2

[5] R. A. Chadwick, G. A. Williams, and D. J. Noy. Co_2 storage: setting a simple bound on potential leakage through the overburden in the north sea basin. *Energy Procedia*, 2017. 1

[6] Jon F. Claerbout. *Imaging the Earth's Interior*. Blackwell Scientific Publications, 1985. 1

[7] dGB Earth Sciences. Netherlands offshore f3 block seismic dataset, 2015. Available at: https://opendtect.org/osr/. 2

[8] dGB Earth Sciences. Penobscot 3d seismic dataset, 2016. Available at: https://opendtect.org/osr/. 2

[9] Shiqi Dong, Xintong Dong, Kaiyuan Zheng, Ming Cheng, Tie Zhong, and Hongzhou Wang. Transformer for seismic image super-resolution, 2024. 5

[10] Ricard Durall, Ammar Ghanim, Mario Fernandez, Norman Ettrich, and Janis Keuper. Deep diffusion models for seismic processing. *Computers & Geosciences*, 2023. 5

[11] Aurélien Gay, Christian Berndt, and Jürgen Mienert. Anomalies in seismic reflectivity as evidence for fluid migration–examples from the mid-norwegian margin. *Marine and Petroleum Geology*, 2006. 1

[12] Michael A Hedderich, Dawei Zhu, and Dietrich Klakow. Analysing the noise model error for realistic noisy label data. In *AAAI*, 2021. 2

[13] Kaggle and TGS. Tgs salt identification challenge dataset, 2019. Available at: https://www.kaggle.com/competitions/tgs-salt-identification-challenge. 2

[14] Chao Li, Sergey Fomel, Yangkang Chen, Robin Dommisse, and Alexandros Savvaidis. Faultvitnet: A vision transformer assisted network for 3d fault segmentation. *Journal of Geophysical Research: Machine Learning and Computation*, 2025. 4

[15] Hendrik Ligtenberg. Detection of fluid migration pathways in seismic data: implications for fault seal analysis. *Petroleum Geoscience*, 2005. 1, 2

[16] Lei Lin, Zhi Zhong, Chuyang Cai, Chenglong Li, and Heng Zhang. Seisgan: Improving seismic image resolution and reducing random noise using a generative adversarial network. *Mathematical Geosciences*, 2023. 5

[17] Fausto Milletari, Nassir Navab, and Seyed-Ahmad Ahmadi. V-net: Fully convolutional neural networks for volumetric medical image segmentation. In *International Conference on 3D Vision*, 2016. 4

[18] J. Reveron and S. Barh. Gas chimneys identification for shallow hazards assessment using seismic attributes. In *Proc. 83rd EAGE Annual Conf. Exh.*, 2022. 1

[19] Etienne Robein. *Seismic imaging: a review of the techniques, their principles, merits and limitations*. Earthdoc, 2010. 1

[20] Phil Schultz. *The seismic velocity model as an interpretation asset*. Society of Exploration Geophysicists, 1998. 2

[21] Jing Wang, Siteng Ma, Yue Liu, and Ruihai Dong. Attention-faultformer: An attention-enhanced 3d cnn & transformer model for seismic fault detection. *Journal of Applied Geophysics*, 2025. 4

[22] Zhiwei Wang, Jiachun You, Wei Liu, and Xingjian Wang. Transformer assisted dual u-net for seismic fault detection. *Frontiers in Earth Science*, 2023. 4

[23] Xinming Wu, Luming Liang, Yunzhi Shi, and Sergey Fomel. Faultseg3d: Using synthetic data sets to train an end-to-end convolutional neural network for 3d seismic fault segmentation. *Geophysics*, 84(3):IM35–IM45, 2019. 4

[24] Oz Yilmaz. *Seismic Data Analysis: Processing, Inversion, and Interpretation of Seismic Data*. Society of Exploration Geophysicists, 2001. 1

[25] Hao Zhang and Wenlei Wang. Imaging domain seismic denoising based on conditional generative adversarial networks (cgans). *Energies*, 2022. 5

[26] Hao-Ran Zhang, Yang Liu, Yu-Hang Sun, and Gui Chen. Seisresodiff: Seismic resolution enhancement based on a diffusion model. *Petroleum Science*, 2024. 5

[27] Yi Zhang, Hongwei Qin, Xiaogang Wang, and Hongsheng Li. Rethinking noise synthesis and modeling in raw denoising. In *CVPR*, 2021. 2